Imaging Technique with Liquid Crystals of Halogen-Containing 3,6-Distyrylpyridazines (= 3,6-Bis(2-phenylethenyl)pyridazines)

by **Thorsten Lifka**, **Peter Seus**, **Annette Oehlhof**, and **Herbert Meier***

Institute of Organic Chemistry, University of Mainz, Duesbergweg 10–14, D-55099 Mainz
(phone: +49 6131 3922605; fax: +49 6131 3925396; e-mail: hmeier@mail.uni-mainz.de)

The 3,6-bis{(1*E*)-2-[4-(dodecyloxy)phenyl]ethenyl}pyridazine (**1a**) was regio- and stereoselectively brominated or chlorinated to the (*Z*,*Z*)-compounds **3** and **6**, respectively. The conjugated core of these systems represents a mesogen for smectic (and nematic) liquid crystals and, moreover, a chromophore with an absorption at the UV/VIS border. Irradiation and efficient intersystem crossing to the triplet state leads to isomerization reactions (*Z*,*Z*) → (*E*,*Z*) in solution as well as in the thermotropic LC phases. Since (*E*,*Z*)-configurations are only tolerated to a very small extent by the mesophases, the photoinduced transition $S \rightarrow N \rightarrow I$ of **6** can be used as an imaging technique.

1. Introduction. – Stilbenoid systems with an extended π conjugation, such as oligo- and poly(1,4-phenylenevinylene)s (= oligo- and poly(1,4-phenyleneethene-1,2-diyl; OPV and PPV), represent a prominent class of compounds in material science. Their tunable chromophores/fluorophores/electrophores permit various applications, for example as electroluminescent and (photo)conductive or nonlinear optical materials (for selected monographs and rewiews, see [1]).

However, apart from some small oligomers, these relatively rigid π systems are barely suitable for the formation of liquid crystals (LCs) [2]. Recently, we found that (*E*,*E*)-3,6-distyrylpyridazines (= 3,6-bis(2-phenylethenyl)pyridazines) **1** with one to three alkoxy groups on the terminal benzene rings represent ideal compounds for the formation of various different liquid crystals: *N*, S_A, S_B, S_C, S_E, $S_{F/I}$, and *Cub*. [3]. We attribute the high tendency of self-organization to the π stacking, the *van der Waals* interaction of the chains and the transversal dipole moment. The first two effects are also valid for the corresponding 1,4-distyrylbenzenes (= 1,4-bis(2-phenylethenyl)benzenes) **2**, but their self-organization tendency is much lower [2–4]. Therefore, the transversal dipole moment seems to be the major effect.

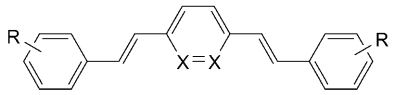

1 X = N
2 X = CH

The N-atoms of the pyridazine ring have still another effect. They bear two (coupled) free electron pairs so that the electronic excitation at long wavelengths

contains $\pi \rightarrow \pi^*$ and $n\_ \rightarrow \pi^*$ transitions [5]. According to *El Sayed*'s rule [6], exothermic singlet–triplet transitions $S(\pi\pi^*) \rightarrow T(n\pi^*)$ and $S(n\pi^*) \rightarrow T(\pi\pi^*)$ are allowed. The 1,4-distyrylbenzenes **2** do not have this ability, and they do not show $E \rightarrow Z$ photoisomerization reactions because the bond order of the olefinic C=C bonds is not lowered enough in the excited singlet state S_1 [1b][7]. In the triplet state of the 3,6-distyrylpyridazines **1**, such isomerization routes are facile [3] and may be used for imaging techniques with liquid crystals.

2. Results and Discussion. – We attempted now to enhance the intersystem-crossing (ISC) rate of 3,6-distyrylpyridazines **1** by the introduction of heavy atoms such as Br- or Cl-atoms. *Scheme 1* shows that the reaction of 3,6-bis{(1*E*)-2-[4-(dodecyloxy)phenyl]ethenyl}pyridazine (**1a**) with Br_2 in AcOH/AcONa yielded the three products **3**–**5** in a ratio of 66:33:1 when 2 mol of Br_2 were used for 1 mol of **1a**. The separation of **3**–**5** was achieved by column chromatography.

Scheme 1

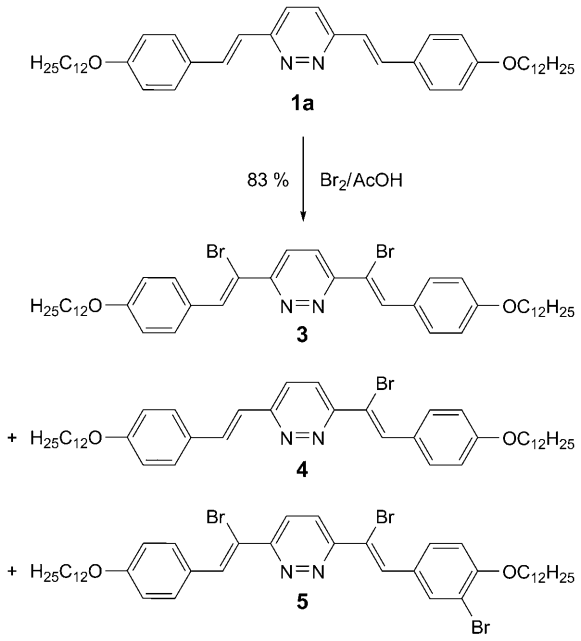

A spontaneous dehydrobromination occurs after the addition of Br_2 to the olefinic C=C bond, *i.e.*, **1a** ((*E*,*E*)) → **3** ((*Z*,*Z*)) and **4** ((*E*,*Z*))[1]. The additional electrophilic

[1]) Addition of Br_2 to (*E*)-stilbene (=1,1′-[(1*E*)-ethene-1,2-diyl]bis[benzene]) yields preponderantly the *meso*-dibromo derivative (*R*,*S*). In the case of (*E*,*E*)-compound **1a**, a mixture of the achiral adducts with configuration (*R*,*S*,*R*,*S*)≡(*S*,*R*,*S*,*R*) and the two chiral enantiomeric adducts with configurations (*S*,*R*,*R*,*S*) and (*R*,*S*,*S*,*R*) can be expected to be the major products. Deprotonation takes then place in α-position to the pyridazine ring because of the electron-withdrawing effect of the heterocyclic ring.

substitution at the electron-rich benzene ring leading to **5** ((*Z*,*Z*)) is a minor side reaction as long as no Br_2 excess is used. The dehydrobromination has obviously a very high regioselectivity since an unsymmetric dibromo compound cannot be observed. However, the question remains whether the Br-substituent is localized at the 'inner' or at the 'outer' olefinic C-atom of **3**. The coupled ^{13}C-NMR spectrum gives the answer. The H-atom-bearing olefinic C-atom leads to a *dt*, which corresponds to the one-bond coupling (^1J) and to a three-bond coupling (^3J) with the two H_o atoms of the neighboring benzene ring. This result is only conform with structure **3**.

The introduction of Cl-atoms into **1a** (→ (*Z*,*Z*)-compound **6**) proved to be more difficult. The direct chlorination with Cl_2 led, by an attack on the olefinic C=C bonds as well as on the aromatic rings, to a scarcely stable mixture of products. Finally we succeeded by application of SO_2Cl_2 as Cl-transfer reagent (*Scheme 2*); however, the yield of the dichloro compound **6** in the (*Z*,*Z*) configuration was rather low (25%).

Scheme 2

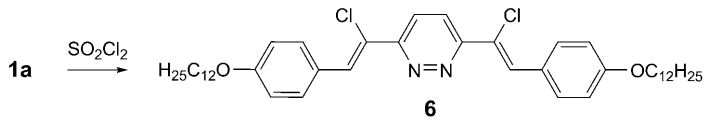

Scheme 3 shows the catalytic hydrogenation of **1a** to **7**, which served for the comparison of the photoactive olefinic systems to a photostable saturated system.

Scheme 3

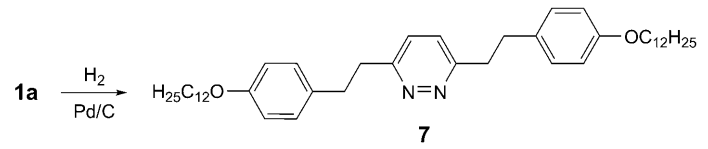

Differential scanning calorimetry (DSC) revealed that the target (*Z*,*Z*)-compound **3** generates a mesophase between 86 and 112°. Compared to the starting (*E*,*E*)-system **1a**, which forms smectic phases [3] between 139 and 266°, the LC temperature range of **3** is better suitable for applications. The mono-brominated compound **4** exhibits phase-transition temperatures, which are lying between those of **1a** and **3**. According to the textures obtained in the polarization microscope, all three compounds **1a**, **3**, and **4** form smectic phases S_C. The hydrogenated compound **7** generates also a smectic phase. Its texture did not permit a more detailed classification. *Fig. 1* summarizes the temperatures *T* and the corresponding enthalpies ΔH for the transitions between crystalline (*Cr*), smectic (*S*), and isotropic (*I*) phases.

The chlorinated (*Z*,*Z*)-compound **6** exhibits a more complex phase behavior. *Fig. 2* shows the DSC cooling curve. Two mesophases can be observed between the crystalline phase (*Cr*) and the isotropic melt (*I*). The peak for the $Cr \rightarrow S_C$ transition has, in the second heating curve of the DSC, a maximum at 129°. The next phase transition $S_C \rightarrow N$ occurs at 137°, and the clearing point $N \rightarrow I$ lies at 139°. Due to the undercooling effect,

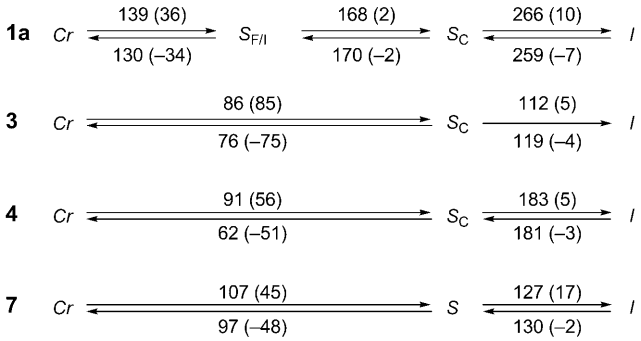

Fig. 1. *Phase transitions of the compounds* **1a**, **3**, **4**, *and* **7**: *onset temperatures [°] of the second heating curves and the first cooling curves.* The numbers in parentheses indicate the enthalpies ΔH in kJmol^{-1}; $\Delta H > 0$ endothermic process, $\Delta H < 0$ exothermic phase transition. A rate of 10 K min^{-1} was used as temperature gradient.

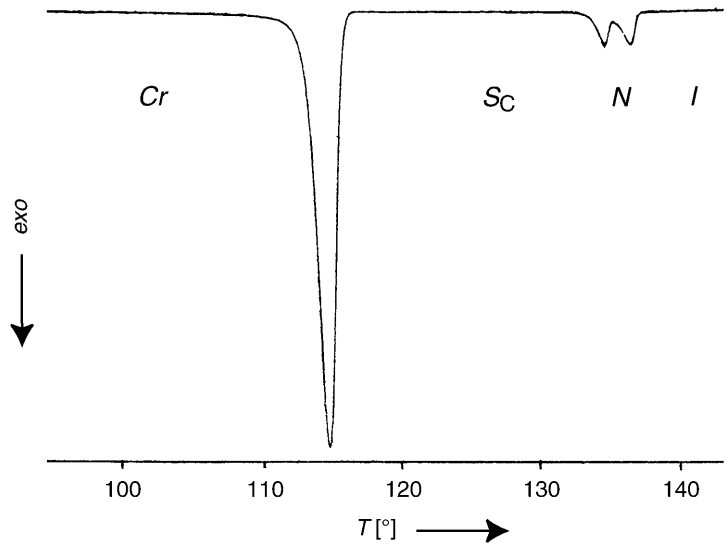

Fig. 2. *DSC Measurement of (Z,Z)-compound* **6**: *second cooling curve measured with a rate of 5 K min^{-1}*

the phase transitions, in particular the crystallization, were observed at lower temperatures in the cooling curve.

The characterization of the LC phases is based on the textures which were obtained with the polarization microscope in a cooling process with a very low temperature gradient of 0.1 K min^{-1}. Under crossed polarizers, the isotropic melt (*I*) appears black. As soon as the first LC phase is formed, color appears due to the birefringence. A light pressure on the phase of **6** causes short 'flashes' in the structureless texture, which are characteristic for a nematic phase *N* in a homeotropic arrangement. Tempering generates then typical nematic droplets (*Fig. 3,a*). A 'schlieren' texture evolves with

beautiful singularities (*Fig. 3,b*). Further cooling leads in a broad temperature range, to the S_C texture (*Fig. 3,c*) until crystallization starts at *ca.* 118° (*Fig. 3,d*). The nematic phase *N* is extremely light-sensitive. Therefore, we used a green filter for its measurements.

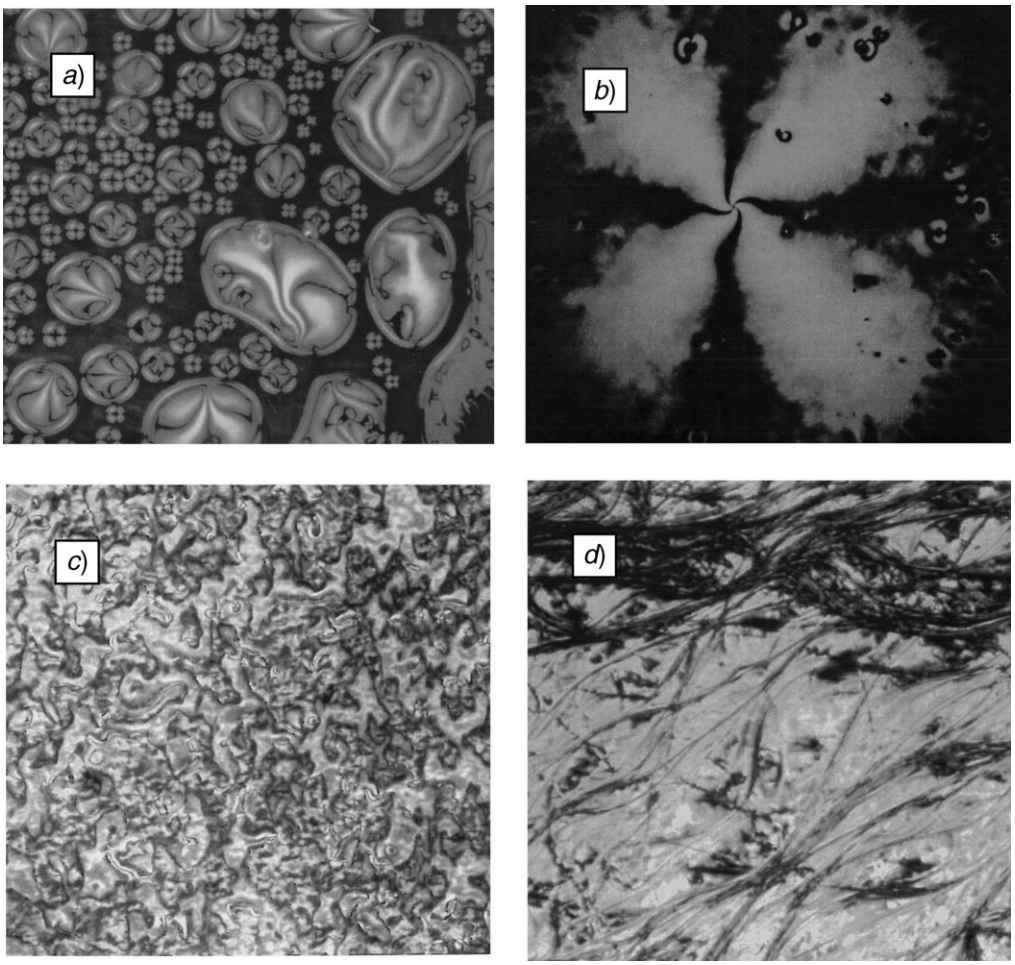

Fig. 3. *Mesophases of* **6** (scale 1:340): a) *nematic droplets,* b) *singularity in the 'schlieren' texture of the nematic phase,* c) *texture of smectic phase* S_C *at 130°, and* d) *starting crystallization at 118°*

(*Z*,*Z*)-Dibromo compound **3** shows a photoisomerization in cyclohexane, which leads fast to the photostationary state of the (*Z*,*Z*) and the less symmetrical (*E*,*Z*) configuration. According to ^{1}H- and ^{13}C-NMR measurements, the presence of the (*E*,*E*)-isomer can be excluded (*Scheme 4*)[2]). The UV/VIS-reaction spectra in *Fig. 4* show the result of an irradiation into the long-wavelength band of **3** ($\lambda \geq 320$ nm). The decrease of this band with a λ_{max} value of 363 nm is attended by an increase of the band

[2]) The detection limit in the ^{1}H-NMR study was below 2%.

between 220 and 300 nm. ^{1}H-NMR Reaction spectra reveal a 50:50 ratio of the (*Z*,*Z*)-compound **3** and its stereoisomer (*E*,*Z*)-**3** in the photostationary state. However, subsequent irradiation of the 1:1 mixture with λ 254 nm shifts the ratio back to a somewhat higher portion of the (*Z*,*Z*)-isomer **3**[3]). The band between 220 and 300 nm decreases then and the band between 300 and 420 nm increases. This wavelength dependance renders the system suitable for an optical switching between states of different (*Z*,*Z*)/(*E*,*Z*) ratio.

Scheme 4. *Photoisomerization of* (Z,Z)*-Compounds* **3** *and* **6** *to Their* (E,Z)*-Isomers* (E,Z)-**3** *and* **6** *and* (E,Z)-**6**, *respectively*

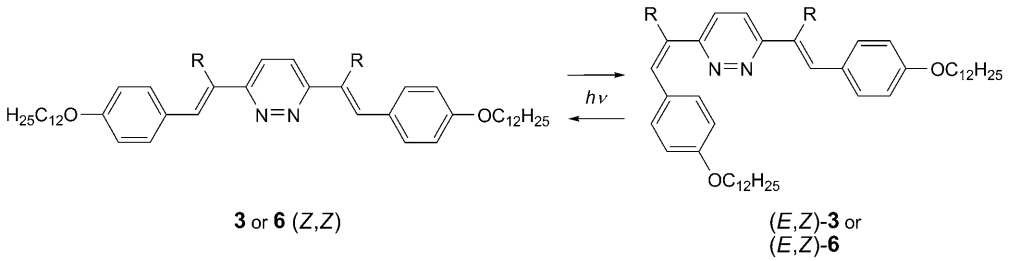

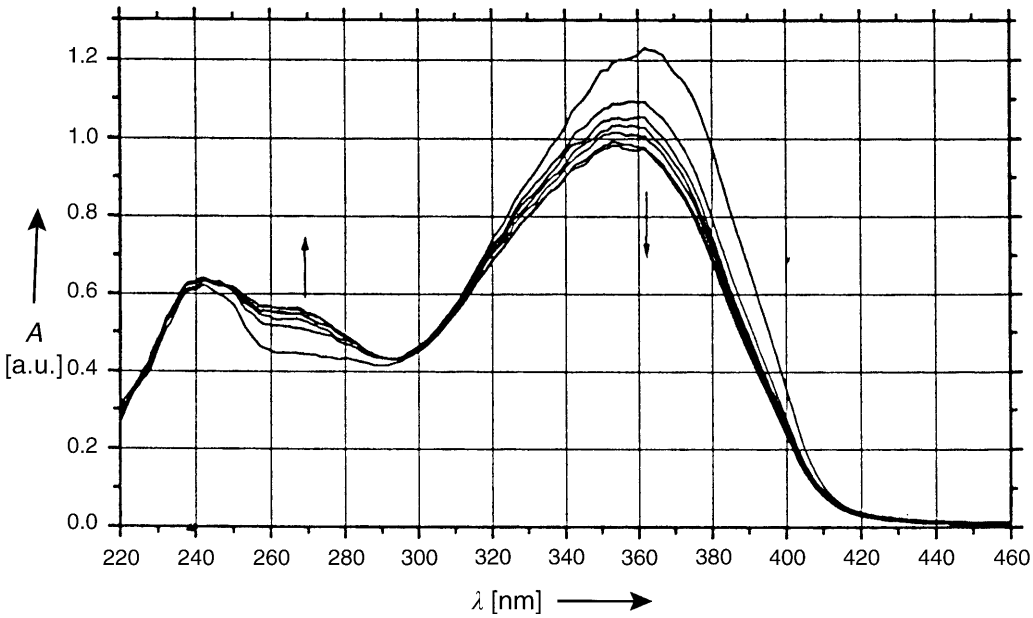

Fig. 4. *UV/VIS Reaction spectra of the irradiation of* (Z,Z)*-compound* **3** *in cyclohexane with* $\lambda \geq 320$ *nm*

The isomer ratio can be easily determined by the integration of the *s* of the olefinic H-atoms in the ^{1}H-NMR spectra ($CDCl_3$): the (*Z*,*Z*)-isomer **3** causes one *s* at δ 8.55 and

[3]) The photostationary state is predominantly determined by the ratio ε(**3**)/ε((*E*,*Z*)-**3**).

(*E*,*Z*)-**3** two *s*, one at δ 7.44 for the '(*E*)-side' and one at δ 8.61 for the remaining '(*Z*)-side'. The *AA'BB'* spin pattern of the aromatic H-atoms is also shifted by the isomerization from δ 6.95 and 7.89 for **3** to δ 6.69 and 6.94 for the '(*E*)-side' and δ 6.94 and 7.87 for the '(*Z*)-side' in (*E*,*Z*)-**3**.

Compared to the photochemical behavior of **1a** and other nonhalogenated 3,6-distyrylpyridazines [3][4], compound **3** exhibits two major advantages: *i*) Due to the enhanced intersystem crossing (ISC), the isomerization process of **3** is much faster. *ii*) The sensitivity of the electronically excited states of **3** toward O_2 is so low that irradiations can be performed in oxygen-containing media.

A certain disadvantage of Br-containing compounds is due to the photochemical C–Br cleavage in long-term irradiations. Therefore, we used compound **6** for the irradiation of the LC phase since the C–Cl bond has a much higher photostability. Irradiations of the nematic phase at 135° led to the isothermal formation of the isotropic melt (*Fig. 5*,*b*). The polychromatic light of the polarization microscope is already sufficient for this change which is based on the photoisomerizaton of the (*Z*,*Z*)-isomer **6** to (*E*,*Z*)-**6** (*Scheme 4*). Irradiations of the smectic phase at 128, 127, 125, 123, 120, and 118° led in all cases to the isothermal formation of the nematic phase (*Fig. 5*,*a*). The rate of the transformation decreased in this sequence of experiments with decreasing temperature. We assume that higher mobility and lower order enhance the chances for the isomerization in the constrained LC medium. We could never observe a direct transformation of the S_C phase to the isotropic phase I. Obviously, the nematic phase *N* tolerates more 'wrong' (*E*,*Z*) configurations than the higher ordered S_C phase.

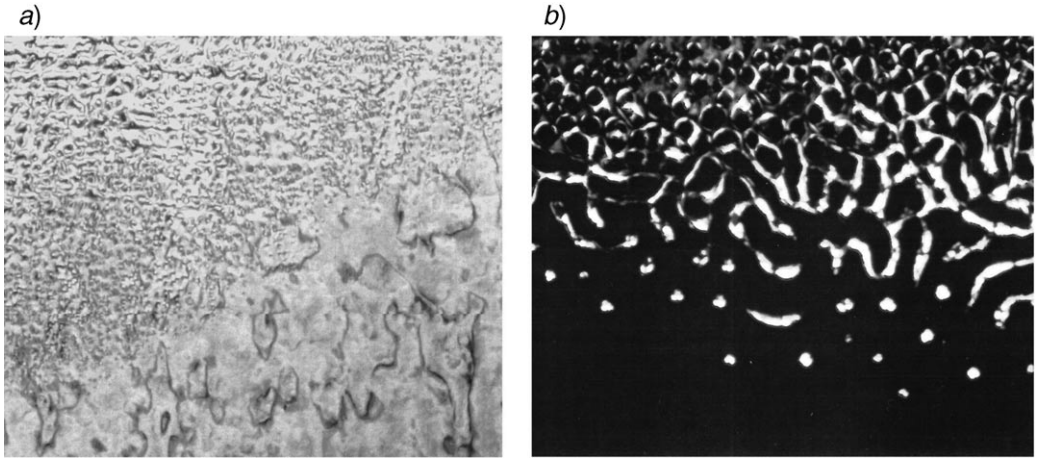

Fig. 5. *Isothermal phase transitions by irradiation of* **6**: a) S_C *phase irradiated at 128.0° on the left upper part so that the nematic phase* N *is formed, and* b) N *phase irradiated so that the formation of the isotropic phase* I (black area) *is started*

The hydrogenated compound **7** does not contain a stilbenoid chromophore. It is photostable in solution as well as in the liquid crystalline state. Compound **1a**, which contains olefinic C=C bonds, shows only in solution the (*E*,*E*) → (*E*,*Z*) isomerization. In the LC state, **1a** is surprisingly photostable [2][3]. The excitation energy can be

transferred to the neighboring mesogens in the self-organized arrangement and finally ends up in heat. We tried to use **7** as an inert host for photoactive guests such as **1a** or **3**. However, phase separation turned out to be a major problem. Finally, we succeeded in preparing a guest–host system of 90% **7** and 10% **1a**. On cooling to 142°, the isotropic mixture formed a smectic phase, and at 132° another smectic phase, until at 99° crystallization started. The textures did not allow to determine the exact type of the *S* phases. A macroscopic phase separation was not discernible. So we irradiated the LC system at 115°. Although an energy transfer from the excited singlet or triplet states of **1a** to **7** can be excluded for energetic reasons, a photoisomerization of **1a** did not occur. Either the constrained medium for the guest molecules **1a** does not permit a photoisomerization or the photostationary state is completely on the (*E*,*E*)-side.

3. Conclusions. – The 3,6-bis{(1*Z*)-1-bromo-2-[4-(dodecyloxy)phenyl]ethenyl}pyridazine (**3**) and 3,6-bis{(1*Z*)-1-chloro-2-[4-(dodecyloxy)phenyl]ethenyl}pyridazine (**6**) can be obtained by halogenation and spontaneous dehydrohalogenation from 3,6-bis{(1*E*)-2-[4-(dodecyloxy)phenyl]ethenyl}pyridazine (**1a**). Both compounds form thermotropic S_C phases, **6** generates additionally a nematic phase *N* in a small temperature range. Irradiation into the long-wavelength band ($\lambda \geq 320$ nm) of the (*Z*,*Z*)-dibromo compound **3** in cyclohexane leads to a photostationary state **3**/(*E*,*Z*)-**3**/(*E*,*E*)-**3** 50:50:0. Subsequent irradiation into the absorption band with higher energy (λ 254 nm) partly reverts the process, so that the (*Z*,*Z*) isomer **3** prevails. A triplet mechanism is assumed for the isomerization routes. Since long-term irradiations of **3** revealed a certain photolability of the C–Br bond, the (*Z*,*Z*)-dichloro compound **6** was used for irradiations of the LC phases. Thereby, isothermal phase transformations $S_C \rightarrow N$ and $N \rightarrow I$ could be observed, which were effected by **6** $\rightarrow$ (*E*,*Z*)-**6** photoisomerization processes. An increase of the (*E*,*Z*)/(*Z*,*Z*) ratio to a certain limit leads to the breakdown of the S_C phase. The *N* phase tolerates some more 'wrong' configuration (*E*,*Z*) until the isotropic melt *I* is generated. To the best of our knowledge, the $S_C \rightarrow N$ process is the first photo-induced transformation between two LC phases [8]. Both irradiation processes can be used as imaging techniques.

We are grateful to the *Deutsche Forschungsgemeinschaft*, the *Fonds der Chemischen Industrie*, and the Materialwissenschaftliches Forschungszentrum der Universität Mainz for financial support.

Experimental Part

1. *General*. CC = Column chromatography. Phase transitions were measured with a differential scanning calorimeter *DSC-7* from *Perkin-Elmer*. UV/VIS: *MCS-224*/*MCS-234* diode array spectrometer from *Zeiss*. Polarization microscopy: *Ortholux II* from *Leitz*. The temp. was regulated with a *FD-52* heating system from *Mettler*. ^{1}H- and ^{13}C-NMR Spectra: *AM-400* spectrometer from *Bruker*; $CDCl_3$ as solvent and Me_4Si as internal standard; δ in ppm and *J* in Hz. FD-MS: *Finnigan-MAT-95* spectrometer. The elemental analyses were performed in the microanalytical department of the Institute of Organic Chemistry of the Unviversity of Mainz.

2. *Bromination of 3,6-Bis{(1*E*)-2-[4-(dodecyloxy)phenyl]ethenyl}pyridazine* (**1a**). Pyridazine **1a** (5.0 g, 7.66 mmol) [3] and AcONa (82 mg, 1.0 mmol) were suspended in AcOH (550 ml) and refluxed, while Br_2 (2.45 g, 15.33 mmol) in AcOH (200 ml) was added dropwise. After 10–20 min refluxing, H_2O (50 ml) was added, and the mixture was extracted with several portions of CH_2Cl_2 until the AcOH phase became colorless. The CH_2Cl_2 extracts were neutralized with aq. Na_2CO_3 soln., washed with H_2O, and

dried ($MgSO_4$). CC (5×60 cm SiO_2, CH_2Cl_2) gave, in this order, **5** (55 mg, 0.8%), **3** (3.42 g, 55%), and **4** (1.51 g, 27%).

Data of 3,6-Bis{(1Z)-1-bromo-2-[4-(dodecyloxy)phenyl]ethenyl}pyridazine (**3**): Yellow crystals which melt after recrystallization from hexane at 86° to the smectic phase S_C. ^{1}H-NMR ($CDCl_3$): 0.89 (*t*, 2 Me); 1.22 (*m*, 32 H, CH_2); 1.45 (*m*, 4 H, CH_2); 1.78 (*m*, 4 H, CH_2); 4.01 (*t*, 2 CH_2O); 6.95, 7.89 (*AA′BB′*, 8 arom. H); 8.00 (*s*, 2 heteroarom. H); 8.55 (*s*, 2 olef. H). ^{13}C-NMR ($CDCl_3$): 14.1 (Me); 22.7, 26.0, 29.2, 29.3, 29.4, 29.6, 31.9 (CH_2, partly superimposed); 68.2 (CH_2O); 114.4, 126.0, 131.8, 133.6 (arom. and olef. CH); 115.7 (olef. C); 127.4, 157.3, 160.0 (arom. C). FD-MS: 810 (100, M^+ (Br_2 isotope pattern)). Anal. calc. for $C_{44}H_{62}Br_2N_2O_2$ (810.8): C 65.18, H 7.71, N 3.46; found: C 65.23, H 7.78, N 3.61.

Data of 3-{(1Z)-1-Bromo-2-[4-(dodecyloxy)phenyl]ethenyl}-6-{(1Z)-2-[4-(dodecyloxy)phenyl]-ethenyl}pyridazine (**4**): Yellow crystals which melt after recrystallization from hexane at 91° to the smectic phase S_C. ^{1}H-NMR ($CDCl_3$): 0.89 (*t*, 2 Me); 1.23 (*m*, 32 H, CH_2); 1.45 (*m*, 4 H, CH_2); 1.78 (*m*, 4 H, CH_2); 4.01 (*m*, 2 CH_2O); 6.92, 7.54 (*AA′BB′*, 4 arom. H (nonbrominated side); 6.94, 7.86 (*AA′BB′*, 4 arom. H (brominated side); 7.22, 7.67 (*AB*, $^3J = 16.3$, 2 olef. H); 7.58, 7.92 (*AB*, $^3J = 8.4$, 2 heteroarom. H); 8.47 (*s*, 1 olef. H); assignments based on INDOR and NOE. ^{13}C-NMR ($CDCl_3$): 14.0 (Me); 22.6, 26.0, 29.2, 29.3, 29.5, 29.6, 31.9 (CH_2, partly superimposed); 68.1, 68.2 (CH_2O); 114.3, 114.9, 122.2, 123.9, 125.6, 128.8, 131.6, 133.0, 134.9 (arom., heteroarom., and olef. CH); 116.2 (CBr); 127.7, 128.7, 156.9, 157.0, 159.9, 160.2 (arom. C). FD-MS: 730 (100, M^+ (Br isotope pattern)). Anal calc. for $C_{44}H_{63}BrN_2O_2$ (731.9): C 72.21, H 8.68, N 3.83; found: 72.04, H 8.48, N 3.94.

Data of 3-{(1Z)-1-Bromo-2-[3-bromo-4-(dodecyloxy)phenyl]ethenyl}-6-{(1Z)-1-bromo-2-[4-(dodecyloxy)phenyl]ethenyl}pyridazine (**5**): Yellow powder. M.p. 93°. ^{1}H-NMR ($CDCl_3$): 0.86 (*t*, 2 Me); 1.27 (*m*, 32 H, CH_2); 1.45 (*m*, 4 H, CH_2); 1.79 (*m*, 4 H, CH_2); 3.99 (*t*, 1 CH_2O); 4.06 (*t*, 1 CH_2O); 6.92, 7.76, 8.18 (*ABC*, 3 arom. H); 6.94, 7.88 (*AA′BB′*, 4 arom. H); 7.99, 8.01 (narrow *AB*, 2 heteroarom. H); 8.48 (*s*, 1 olef. H, 1 H); 8.56 (*s*, 1 olef. H). ^{13}C-NMR ($CDCl_3$): 14.1 (Me); 22.7, 26.0, 29.0, 29.2, 29.3, 29.6, 29.9 (CH_2, partly superimposed); 68.2, 69.3 (CH_2O); 112.1, 115.2, 116.9 (CBr); 112.4, 114.4, 126.0, 126.1, 130.8, 131.8, 132.3, 133.9, 134.6 (arom., heteroarom., and olef. CH); 127.5, 128.8, 156.1, 157.0, 157.6, 160.1 (arom. and heteroarom. C). Due to the very low yield of this by-product, we refrained from further characterizations.

3. *Chlorination of* **1a** *to 3,6-Bis{(1Z)-1-chloro-2-[4-(dodecyloxy)phenyl]ethenyl}pyridazine* (**6**). Pyridazine **1a** (5.0 g, 7.66 mmol) was suspended at 77° in dry CCl_4 (100 ml). A soln. of SO_2Cl_2 (1.0 g, 7.41 mmol) in dry CCl_4 (50 ml) was added dropwise. Several small portions of dibenzoyl peroxide were added to the boiling mixture. The originally yellow color turned orange, and the suspended particles dissolved. When the generation of SO_2 ceased, the mixture was cooled to r.t. and washed with aq. Na_2CO_3 soln. and H_2O. Evaporation of the solvent gave an orange residue. TLC (SiO_2, CH_2Cl_2): three products with R_f 0.3, 0.5, and 0.65, the latter corresponding to **6** as major product. Recrystallization of the orange residue from CH_2Cl_2 and then from hexane yielded yellow needles of **6** (1.40 g, 25% rel. to **1a**), which melted at 129° to the smectic S_C phase. An equimolar or excess amount of SO_2Cl_2 cannot be recommended to get highly pure **6** (*Z*,*Z*). ^{1}H-NMR ($CDCl_3$): 0.86 (*t*, 2 Me); 1.26 (*m*, 32 H, CH_2); 1.43 (*m*, 4 H, CH_2); 1.78 (*m*, 4 H, CH_2); 3.99 (*t*, 2 CH_2O); 6.94, 7.87 (*AA′BB′*, 8 arom. H); 7.96 (*s*, 2 heteroarom. H). ^{13}C-NMR ($CDCl_3$): 14.1 (Me); 22.7, 26.1, 29.3, 29.4, 29.6, 29.7, 31.9 (CH_2, partly superimposed); 68.2 (CH_2O); 114.6, 124.0, 124.1, 126.9, 129.7, 132.1, 156.3, 160.0 (arom., heteroarom., and olef. C). FD-MS: 720 (100, M^+ (Cl_2 isotope pattern)). Anal. calc. for $C_{44}H_{62}Cl_2N_2O_2$ (721.9): C 73.21, H 8.66, N 3.88; found: C 73.09, H 8.52, N 3.96.

4. *Hydrogenation of* **1a** *to 3,6-Bis{2-[4-(dodecyloxy)phenyl]ethyl}pyridazine* (**7**). A suspension of **1a** (200 mg, 0.3 mmol) and 10% Pd/C (22 mg)) in dry DMF (70 ml) was stirred at 110° under a pressure of 3.0 bar ($3 \cdot 10^5$ Pa) H_2 for 18 h. H_2O (600 ml) was added, and the mixture was extracted with CH_2Cl_2 ($3 \times$ 50 ml). Concentration of the dried ($MgSO_4$) org. phase gave a residue, which was twice recrystallized from hexane. Colorless needles of **7** (120 mg, 60%) were obtained which melted at 88° to the smectic phase. ^{1}H-NMR ($CDCl_3$): 0.86 (*t*, 2 Me); 1.24 (*m*, 32 H, CH_2); 1.42 (*m*, 4 H, CH_2); 1.74 (*m*, 4 H, CH_2); 3.02, 3.19 (*AA′BB′*, 8 H, CH_2CH_2 (linker)); 3.90 (*t*, 2 CH_2O); 6.78, 7.05 (*AA′BB′*, 8 arom. H); 6.97 (*s*, 2 heteroarom. H). ^{13}C-NMR ($CDCl_3$): 14.1 (Me); 22.7, 26.1, 29.3, 29.4, 29.4, 29.6, 29.6, 29.6, 29.7, 31.9 (CH_2); 68.1 (CH_2O); 34.7, 38.0 (CH_2 (linker)); 114.6, 126.3, 129.4 (arom. and heteroarom. CH); 132.8,

157.6, 160.8 (arom. and heteroarom. C). EI-MS: 656 (48, M^+), 655 (100), 487 (21), 107 (96), 57 (43), 43 (48). Anal. calc. for $C_{44}H_{68}N_2O_2$ (657.0): C 80.43, H 10.43, N 4.26; found: C 80.08, H 10.41, N 4.16.

5. *Irradiation in Solution.* A $0.5 \cdot 10^{-4}$ M soln. of (*Z,Z*)-compounded **3** in cyclohexane (6.5 mg in 160 ml) was irradiated at r.t. with a *Hanovia-450-W* medium pressure mercury lamp equipped with a *Duran* glass filter ($\lambda \geq 320$ nm). The soln. was rigorously stirred, or N_2 was purged through the soln., so that the soln. was continously exchanged in the irradiation zone (monitoring by UV/VIS). As soon as the photostationary state was reached, the soln. was concentrated, and the residue dissolved in $CDCl_3$. ^{1}H-NMR: several integrations of the signals of the olef. H-atoms and independently of the arom. H-atoms (see *General Part*) were averaged and gave the ratio **3**/(*E,Z*)-**3** 50:50. The presence of (*E,E*)-**3** could be excluded with a margin of error of $\leq 2\%$.

When the soln. which represented the photostationary state was irradiated with λ 254 nm (low-pressure mercury lamp), the portion of (*Z,Z*)-isomer **3** was enriched from 50 to *ca.* 85% in the new photostationary state. Irradiations with λ 254 nm or $\lambda \geq 320$ nm over a period of 48 h led to a partical cleavage of the C–Br bonds and to a cross-linking of the material (fatigue effect).

6. *Irradiation of the LC Phases.* Compound **6** or the mixtures **7**/**1a** or **7**/**6** 10:1 were molten to their isotropic phase and studied in the polarization microscope by using the unfiltered polychromatic light of the microscope or by additional irradiation with λ 366 nm. A low temp. gradient yielded the desired temp. ranges at 135, 128, 127, 125, 123, 120, and 118° with an accuracy of ± 0.3 K. The textures were then photographed with a *400-ASA-Kodak-Ektachrom* film.

REFERENCES

[1] a) H.-H. Hörhold, M. Helbig, D. Raabe, J. Opfermann, U. Scherf, R. Stockmann, D. Weiß, *Z. Chem.* **1987**, *27*, 126; b) H. Meier, *Angew. Chem.* **1992**, *104*, 1425; *Angew. Chem., Int. Ed.* **1992**, *31*, 1399; c) K. Müllen, *Pure Appl. Chem.* **1993**, *65*, 89; d) W. R. Salaneck, I. Lundström, B. Ranby, 'Conjugated Polymers and Related Materials', Oxford University Press, Oxford, 1993; e) J. M. Tour, *Chem. Rev.* **1996**, *96*, 537; f) A. Kraft, A. C. Grimsdale, A. B. Holmes, *Angew. Chem.* **1998**, *110*, 416; *Angew. Chem., Int. Ed.* **1998**, *37*, 403; g) K. Müllen, G. Wegner, 'Electronic Materials: The Oligomer Approach', Wiley–VCH, Weinheim, 1998; h) U. Scherf, *Top. Curr. Chem.* **1999**, *201*, 163; i) R. E. Martin, F. Diederich, *Angew. Chem.* **1999**, *111*, 1440; *Angew. Chem., Int. Ed.* **1999**, *38*, 1350; j) J. L. Segura, N. Martín, *J. Mater. Chem.* **2000**, *10*, 2403; k) G. Hadziioannou, P. F. van Hutten, 'Semiconducting Polymers', Wiley–VCH, Weinheim, 2000; l) H. Meier, *Angew. Chem.* **2005**, *117*, 2536; *Angew. Chem., Int. Ed.* **2005**, *44*, 2482; m) H. Meier, in 'Carbon-Rich Compounds', Eds. M. M. Haley and R. R. Tykwinski, Wiley–VCH, Weinheim, 2006, pp. 476–528; n) A. C. Grimdsdale, in 'Organic Light-Emitting Devices' Eds. K. Müllen and U. Scherf, Wiley–VCH, Weinheim, 2006, pp. 215–243.

[2] H. Meier, T. Lifka, U. Stalmach, A. Oehlhof, S. Prehl, *Eur. J. Org. Chem.* **2008**, 1568, and refs. cit. therein.

[3] T. Lifka, G. Zerban, P. Seus, A. Oehlhof, H. Meier, *Tetrahedron* **2008**, *64*, 6551.

[4] G. Zerban, H. Meier, *Z. Naturforsch., B* **1993**, *48*, 171.

[5] H. Meier, publication in preparation.

[6] M. A. El-Sayed, *J. Chem. Phys.* **1962**, *36*, 573.

[7] K. Sandros, M. Sundahl, O. Wennerström, U. Norinder, *J. Am. Chem. Soc.* **1990**, *112*, 3082.

[8] H. Meier, U. Stalmach, M. Fetten, P. Seus, M. Lehmann, C. Schnorpfeil, *J. Inf. Recording* **1998**, *24*, 47.

Received June 26, 2008